Development/Plasticity/Repair

SECISBP2L-Mediated Selenoprotein Synthesis Is Essential for Autonomous Regulation of Oligodendrocyte Differentiation

Zhong-Min Dai,[1*] Wei Guo,[1*] Dan Yu,[1] Xiao-Jing Zhu,[1,2] Shuhui Sun,[1] Hao Huang,[1] Min Jiang,[1] Binghua Xie,[1] Zunyi Zhang,[1] and Mengsheng Qiu[1]

[1]Institute of Life Sciences, Key Laboratory of Organ Development and Regeneration of Zhejiang Province, College of Life Sciences, Hangzhou Normal University, Hangzhou, Zhejiang 311121, People's Republic of China, and [2]The Affiliated Hospital, Hangzhou Normal University, Hangzhou, Zhejiang 310015, People's Republic of China

Thyroid hormone (TH) controls the timely differentiation of oligodendrocytes (OLs), and its deficiency can delay myelin development and cause mental retardation. Previous studies showed that the active TH T3 is converted from its prohormone T4 by the selenoprotein DIO2, whose mRNA is primarily expressed in astrocytes in the CNS. In the present study, we discovered that SECISBP2L is highly expressed in differentiating OLs and is required for DIO2 translation. Conditional knock-out (CKO) of Secisbp2l in OL lineage resulted in a decreased level of DIO2 and T3, accompanied by impaired OL differentiation, hypomyelination and motor deficits in both sexes of mice. Moreover, the defective differentiation of OLs in Secisbp2l mutants can be alleviated by T3 or its analog, but not the prohormone T4. The present study has provided strong evidence for the autonomous regulation of OL differentiation by its intrinsic T3 production mediated by the novel SECISBP2L-DIO2-T3 pathway during myelin development.

Key words: **Dio2; myelin; oligodendrocyte; Secisbp2l; selenoprotein; thyroid hormone**

Significance Statement

Secisbp2l is specifically expressed in differentiating oligodendrocytes (OLs) and is essential for selenoprotein translation in OLs. Secisbp2l regulates Dio2 translation for active thyroid hormone (TH) T3 production in the CNS. Autonomous regulation of OLs differentiation via SECISBP2L-DIO2-T3 pathway.

Introduction

Thyroid hormone (TH) plays an important role in the development of myelin in the CNS, and deficiency in TH is frequently associated with mental retardation in children. Thyroxine (T4) was initially found to be able to accelerate myelinogenesis in 1966 (Hamburgh, 1966), and later studies demonstrated that TH is required for the timely differentiation of oligodendrocytes (OLs), the myelin-forming cells in the CNS (Barres et al., 1994; Baas et al., 2002; Billon et al., 2002; Sharlin et al., 2008; Calzà et al., 2010; Dugas et al., 2012; Picou et al., 2012; Vose et al., 2013; Baxi et al., 2014; Lee and Petratos, 2016; Bernal, 2017).

The circulating TH level is primarily maintained by a negative feedback loop (Dumitrescu and Refetoff, 2013). While excess TH suppresses the production of thyrotropin-releasing hormone from the hypothalamus, a decrease of TH elevates thyrotropin-releasing hormone expression and stimulates the synthesis and release of thyroid-stimulating hormone from the pituitary, which in turn stimulates the production and release of T4 from thyroid gland (Dumitrescu and Refetoff, 2013). Under physiological conditions, T4 level exceeds nearly two orders of magnitude that of T3 in circulatory system (Bianco and Kim, 2006). Circulating T4 is subsequently converted into active T3 by locally expressed deiodinase 1 (DIO1) and DIO2 in tissues requiring a high concentration of T3, which binds to the TH receptors THRa and THRb and activates the transcription of downstream target genes. In contrast, DIO3 antagonize the TH pathway as it converts T4 into inactive rT3 or T3 into inactive T2 (Bianco and Kim, 2006; Dumitrescu and Refetoff, 2013). Given that mRNA of Dio2 but not Dio1 is detectable in the CNS, the majority of T3 in the CNS

Received Oct. 27, 2021; revised June 9, 2022; accepted June 11, 2022.

Author contributions: Z.-M.D. and M.Q. designed research; Z.-M.D., W.G., D.Y., X.-J.Z., S.S., H.H., M.J., and B.X. performed research; Z.Z. contributed unpublished reagents/analytic tools; Z.-M.D., W.G., D.Y., X.-J.Z., S.S., H.H., M.J., B.X., and M.Q. analyzed data; Z.-M.D. wrote the first draft of the paper; Z.-M.D. and M.Q. edited the paper; Z.-M.D. and M.Q. wrote the paper.

This work was supported by the Ministry of Science and Technology China Brain Initiative Grant 2022ZD0204701; the National Natural Science Foundation of China Grants 31871480, 81771028, and 32170969; and by the Key medical disciplines of Hangzhou.

*Z.-M.D. and W.G. are joint first authors.

The authors declare no competing financial interests.

Correspondence should be addressed to Mengsheng Qiu at m0qiu001@yahoo.com.

https://doi.org/10.1523/JNEUROSCI.2141-21.2022

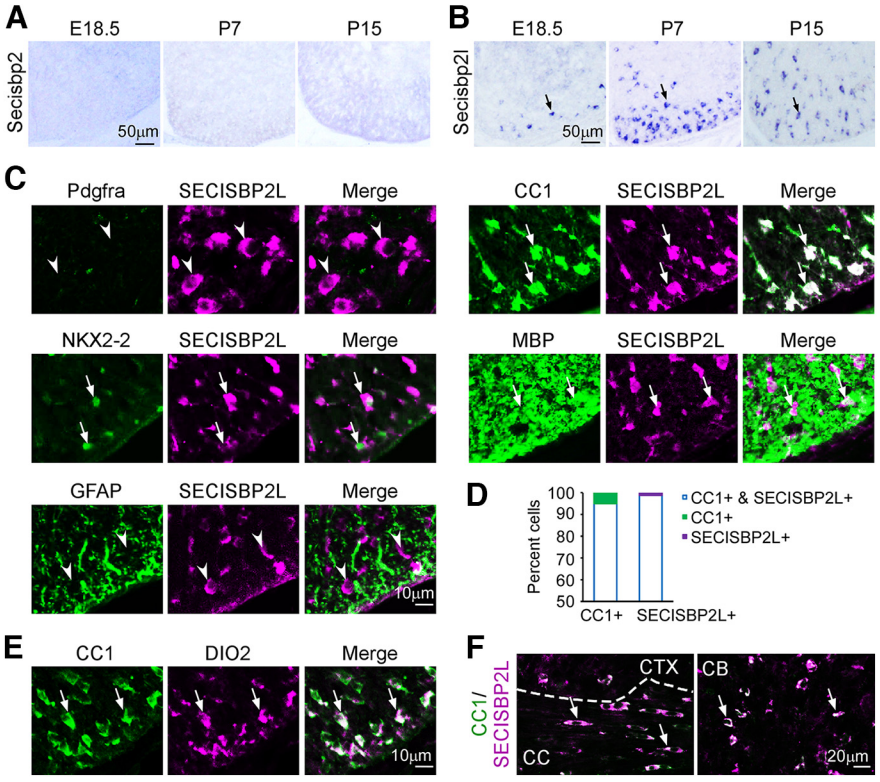

Figure 1. Selective expression of Secisbp2l in OLs during differentiation stage. ***A***, ***B***, ISH revealed that Secisbp2l, but not Secisbp2, is expressed in the white matter of spinal cord from E18.5 to P15. Secisbp2l+ cells are represented by arrows. ***C***, SECISBP2L is co-localized with CC1 and NKX2-2 (arrows), but not with Pdgfra (arrowheads) and GFAP. Immunofluorescent staining (IF) was performed on spinal cord transverse sections at P7 for all markers except for Pdgfra, which is pseudo-colored from ISH image. ***D***, Relative ratio of SECISBP2L and CC1-positive cells. ***E***, Co-labeling of DIO2 with CC1 in P7 spinal cord (represented by arrows). ***F***, Co-labeling of SECISBP2L with CC1 in cortex (CTX), corpus callosum (CC), and cerebellum (CB) at P15. Double positive cells appear as white (arrows).

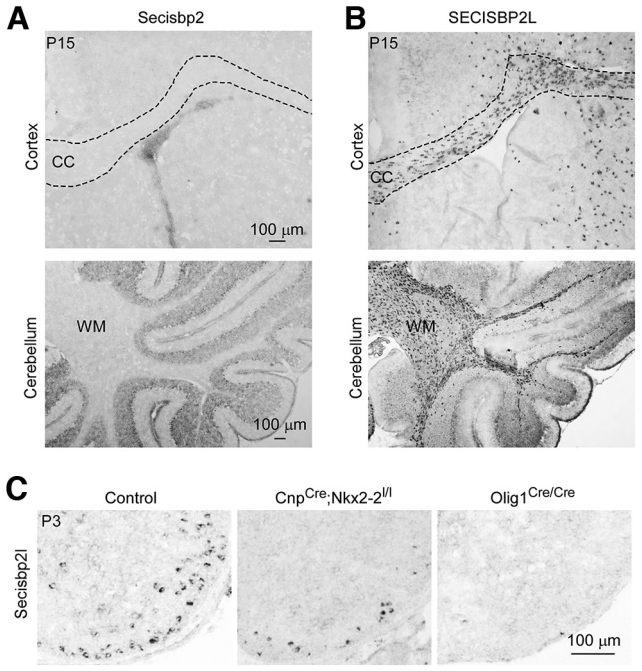

Figure 2. Secisbp2l, but not Secisbp2, is expressed in NFOs. ***A***, ISH revealed the lack of Secisbp2 expression in cortical and cerebellar OLs. ***B***, Immunohistochemical staining of SECISBP2L in the white matter OLs in the cerebral cortex and cerebellum. ***C***, Reduced expression of Secisbp2l in the spinal cord white matter of Nkx2.2 CKO and Olig1−/− mutants.

is thought to be locally produced by DIO2 expressing astrocytes (Guadaño-Ferraz et al., 1997, 1999).

Interestingly, all three DIOs belong to selenoproteins which are featured by their mRNAs containing at least one in-frame UGA codon in the coding sequence and a selenocysteine (Sec) insertion sequence (SECIS) which forms a hairpin-like structure in the 3′ untranslated region (Kryukov et al., 2003). The UGA "stop codon" could be translated into Sec, the 21st amino acid, by SECIS binding protein 2 (SECISBP2) in association with $tRNA^{Sec}$ and selenoprotein specific elongation factor eEFSec (Kryukov et al., 2003). Although SECISBP2-like (SECISBP2L), the paralog of SECISBP2 in vertebrate, capable of binding to SECIS elements, all the previous studies demonstrated that it is unable to carry out UGA to Sec translation (Copeland et al., 2000, 2001; Donovan and Copeland, 2009, 2012). Given that DIO2 functions only if the UGA "stop codon" was translated, it would be important and necessary to investigate the cellular distribution and functional involvement of SECISBP2 and SECISBP2L during myelin development.

In this study, we report that Secisbp2l, but not Secisbp2, is selectively expressed in newly formed OLs (NFOs) in the developing brain and spinal cord tissues. Molecular and biochemical studies revealed that mouse SECISBP2L protein can directly bind to DIO mRNAs and promote their translation. More importantly, we demonstrated that a DIO2-dependent endogenous production of T3 in OPCs is required for the timely differentiation of OLs and subsequent myelinogenesis. Collectively, our studies have provided both the *in vitro* and *in vivo* evidence for a novel molecular pathway for the autonomous regulation of OL differentiation and myelin development.

Materials and Methods

Animals

Use of the animals was approved by the Committee of Laboratory Animals, Hangzhou Normal University. Mouse lines for FLPeR (stock #003946; Farley et al., 2000) and $Olig1^{Cre}$ (stock #011105; Lu et al., 2002) were obtained from The Jackson Laboratory. For generation of $Secisbp2l^{loxP/loxP}$ CKO targeting vector, Secisbp2l exon3 and its flanking sequence was PCR amplified from 129 mouse genomic DNA by Sbp2l-Ex3F (gcttgatatccatatgTGGGCTGTTGTAATCTGGAC) and Sbp2l-Ex3R (gctggaattcggcgcgccGTGTTGGCATTGTCACTGTAC) and ligated into the EcoRV and EcoRI sites of the CKO1 vector. The 3′ arm sequence was amplified by primer pair of Sbp2l-3armF (gttatattaagggttccggatccGTGGTTAAATGTCACTGTACC) and Sbp2l-3armR (ggctcgaaacccgcggatcCCTTGCCTTTAACACCAGCTC), and cloned into the BamHI site using T4 DNA polymerase (Sun et al., 2015), while the 5′ arm sequence was amplified by Sbp2l-5armF (tagggcgaattgggtactaattaaATCTCACGCCCCATTCATCC) and Sbp2l-5armR (cgacctaggaattcttaaggtaccAGTCTGTGCACAATGCTCACACTGT), and cloned

into the KpnI and PacI sites. The Secisbp2l$^{loxP/loxP}$ CKO targeting vector was electroporated into mouse embryonic stem cells for screening, and chimeric mice were produced with the mutant ES clones. The offspring mice were genotyped using primers of Sbp2l-ckoF (CCCTCTTGTTT GAAAGTGTA) and Sbp2l-ckoR (GGCTTCATCCCTTACTTGTT), which generated the 322- and 395-bp band for wild-type (WT) and loxP flanked exon3, respectively. Neo cassette was then removed by crossing with FLPeR mice. Deletion of exon3 of Secisbp2l by Olig1^{Cre} results in conditional knock-out (CKO) of Secisbp2l in OLs (Olig1^{Cre};Secisbp2l$^{l/l}$). T4 and GC-1 (also named as Sobetirome, Sigma-Aldrich #SML1900) were injected intraperitoneally into mice from P0 to P2 at a dose of 9 ng/g body weight. Mice of either sex were used for sampling.

Generation of antibodies against Secisbp2l and Dio2 proteins

The C-terminal 257-aa encoding sequence of mouse Secisbp2l (C257-Sbp2l) was amplified by primers tgccgcgcggcagccatatgAGGAGCGT GAAGACGGTGCC and ctttgttagcagccggatccTTATGTACTTTGGGGA GGAG, and cloned into NdeI and BamHI sites of pET15b (Novagen) using T4 DNA polymerase for His-tagged bacterial expression system (Sun et al., 2015). The pET15b-C257-Sbp2l plasmid was transformed into Rosetta (DE3; Novagen), the picked colony was then cultured to an OD600 > 1 and expression of C257-Sbp2l was induced by adding IPTG to 0.1 mM and shaking overnight at room temperature. C257-Sbp2l fragment was purified by Ni-NTA 1 ml (Pre-Packed Gravity Column; Sangon Biotech) under native condition. The purified C257-Sbp2l was used as an antigen for antibody production in rabbits (Sangon Biotech).

Because of the low expression level of Dio2, a homemade pET-EGFP-3C vector was used instead of pET15b for the Dio2 antigen expression. The 100-aa encoding sequence was amplified by primers cttgaagtccttttttcagggtccgaagCTTTTCACTAGGCAACTGCCAGC and tg gtgctcgagtgcggccgcttaTCTCTGCACGATGCACACACGT, and cloned into HindIII and NotI site of pET-EGFP-3C. The resulting plasmid pET-EGFP-3C-Dio2 was transformed into Rosetta (DE3) for expression. After IPTG induction, the bacterial expressed EGFP-3C-Dio2 protein has a weak fluorescence and was almost insoluble. The EGFP-3C-Dio2 was dissolved in 8 M urea for Ni-NTA binding, and purified under denaturation condition. The purified EGFP-3C-Dio2 was dialyzed by a serial of 4, 2, 1, and 0 M urea in TBS buffer. The dialyzed EGFP-3C-Dio2 was soluble and used as antigen for rabbit anti-Dio2 antibody production (Sangon Biotech).

In situ *hybridization (ISH) and immunostaining*

Samples were fixed in 4% paraformaldehyde/PBS (PFA) at 4°C overnight, followed by 20% sucrose infusion, and finally embedded in Tissue-Tek O.C.T Compound (Sakura Finetek) for cryosection. Samples were cryo-sectioned at 18 μm for ISH. Standard ISH was performed according to manufacturer's instruction. For fluorescent immunostaining, tissues were sectioned on a cryostat (14 μm thick), and cultured cells were fixed with 4% PFA for 30 min at room temperature. The primary antibodies used for immunostaining are as follows: anti-OLIG2 (Millipore, MABN50, 1:1000), anti-MAG (Millipore, MAB1567, 1:500), anti-CC1 (Abcam, ab16794, 1:500), anti-GFAP (Millipore, ab9610, 1:2000), anti-NKX2.2 (Developmental Studies Hybridoma Bank, 74.5A5, 1:50), anti-MBP (Abcam, ab7349, 1:500).

RNA-sequencing

Spinal cord tissues at postnatal day (P)7 were obtained from WT, Olig1^{Cre}; Secisbp2l$^{L/L}$ mice,

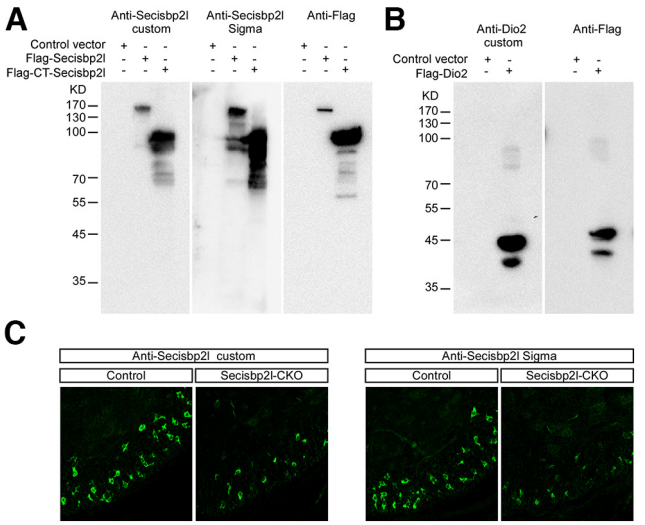

Figure 3. Verification of Anti-SECISBP2L and Anti-DIO2 antibodies. ***A***, ***B***, Flag-tagged Secisbp2l, CT-Secisbp2l, or Flag-eGFP-Dio2 or control vector plasmids were transfected into HEK293T cells. Cell lysates were subjected to Western blotting with anti-Flag, custom-made anti-SECISBP2L, or commercial anti-SECISBP2L antibody (Sigma Prestige, Human Protein Atlas Number: HPA039875) or anti-DIO2 antibodies. An identical banding pattern detected by anti-Flag and anti-Secisbp2l or anti-Dio2 confirms the specificity of these antibodies. ***C***, Immunofluorescent staining also showed a similar expression pattern in P3 spinal tissue with our custom-made anti-SECISBP2L and commercial anti-SECISBP2L antibody.

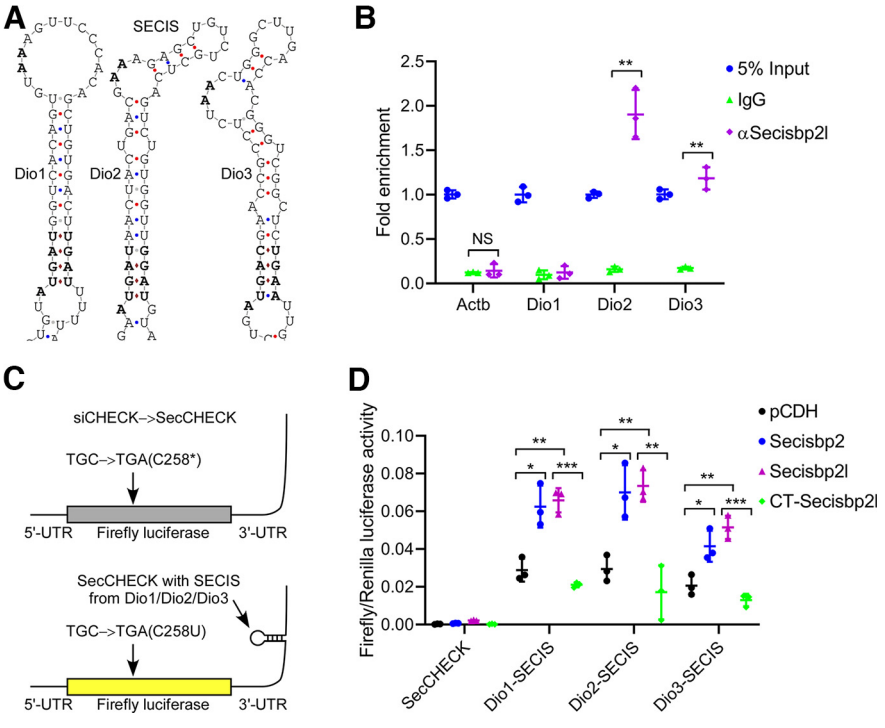

Figure 4. Secisbp2l is able to promote translation of DIOs. ***A***, SECIS elements of mouse Dios. Highly conserved nucleotides are indicated in bold. ***B***, Enrichment of Dio2 and Dio3 mRNA by anti-SECISBP2L antibody by co-immunoprecipitation. Note that Ct values for Dio1 exceeded 35, indicating an extremely low expression of Dio1. Actb (β-actin) was used as a negative control. ***C***, Scheme of SecCHECK with SECIS from Dio1, Dio2, and Dio3. Mutation of a TGC codon in firefly luciferase of siCHECK into TGA results in SecCHECK. ***D***, SecCHECK with or without SECIS were co-transfect with control vector (pCDH), Secisbp2, full-length Secisbp2l or C-terminal Secisbp2l (CT-Secisbp2l) for luciferase activity assay. Overexpression of Secisbp2l and Secisbp2 increased firefly luciferase activity with SECIS, whereas CT-Secisbp2l had little effect. All values are represented as mean ± SD; *$p < 0.05$, **$p < 0.01$, ***$p < 0.001$; NS, not significant.

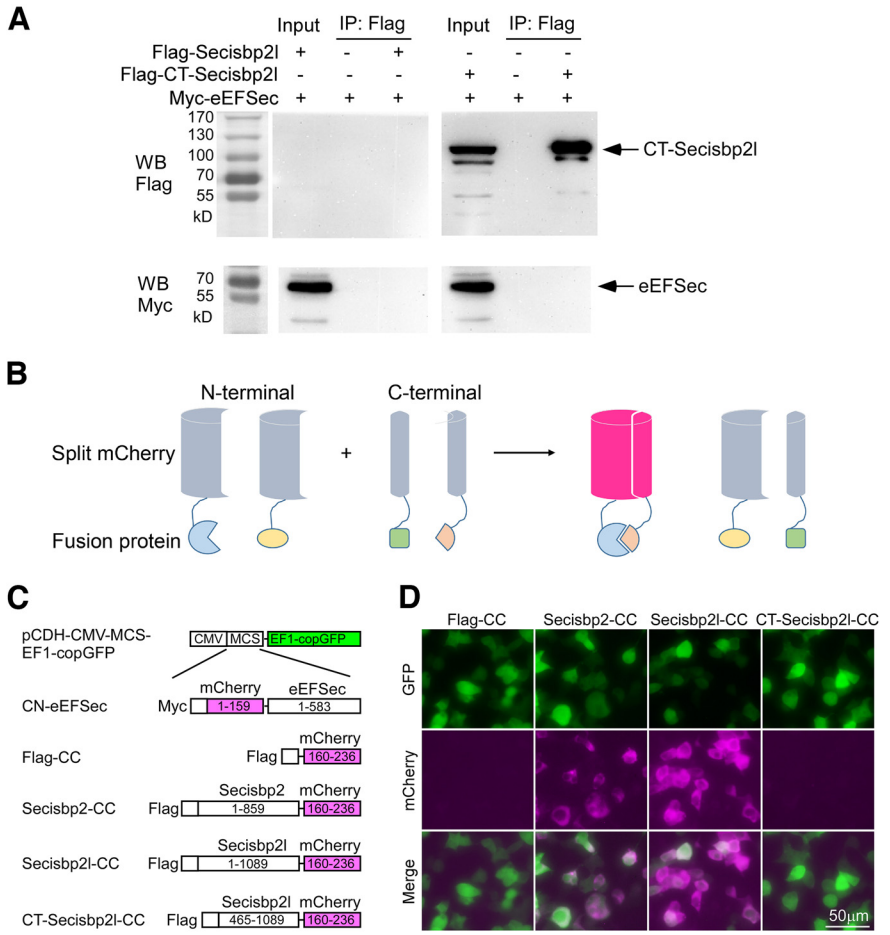

Figure 5. Full-length Secisbp2l but not CT-Secisbp2l interact with eEFSec. ***A***, eEFSec was not co-immunoprecipitated with CT-Secisbp2l. Expression of full-length Secisbp2l (Flag-Secisbp2l) was undetectable. ***B***, Strategy of detecting protein-protein interactions by split mCherry. When the fusion proteins interact with each other, the split mCherry restores its fluorescence. ***C***, Scheme of fusion constructs used for split mCherry experiments. Note that the protein size was not scaled proportionally. ***D***, CN-eEFSec was co-transfected with constructs encoding various Secisbp2l fragments. Only the full-length but not the CT-Secisbp2l interacts with eEFSec and restored mCherry activity. GFP expression regulated by an independent promoter was used as an internal control. Exposure time for capturing GFP and mCherry images was 40 ms and 1 s, respectively.

immersed in RNAstore solution (CWBiotech) and stored in −80°C before RNA isolation. Total RNA was purified using TRIzol reagent (Sangon Biotech). For construction of sequencing libraries, 1 μg of total RNA was used with VAHTS mRNA-seq V2 Library Prep kit for Illumina (Vazyme Biotech). Sequencing was performed by Sangon Biotech (Shanghai) Co, Ltd. using Illumina Hiseq 2500 (Illumina). The sequencing data were submitted to gene expression omnibus under the accession number of GSE119359.

Luciferase report assay

For luciferase activity assay, the full-length 1089 and the C-terminal 624-aa encoding sequences of Secisbp2l from mouse were separately PCR amplified and cloned into pCDH-CMV-MCS-EF1-copGFP (pCDH) vector (System Biosciences) by T4 DNA polymerase. The SECIS sequences from mouse Dio1, Dio2, and Dio3 were cloned into the XbaI site of the SecCHECK vector modified from siCHECK (Promega; Sun et al., 2015). Each 250 ng of SecCHECK with or without SECIS was mixed with 250 ng of pCDH, pCDH-Secisbp2l, or pCDH-CT- Secisbp2l, and transfected into HEK293T cells in 24 wells. Luciferase activity was measured using a Dual-Luciferase Reporter Assay System (Promega).

Cell culture assay

For lentivirus production, pCDH or pCDH-Secisbp2l was mixed with psPAX2 and pMD2.G (4:3:1) to transfect HEK293T cells. The plasmids pMD2.G and psPAX2 were gifts from Didier Trono (Addgene plasmid #12259 and #12260, respectively). The transfected HEK293T cells were cultured in DMEM-F12 + 10% FBS for 48 h. The medium with lentivirus was filtered through 0.45-μm filters, and each 30 ml of the filtered virus solution was mixed with 7.5 ml of 5× PEG8000/NaCl solution containing 40% (w/v) PEG8000 and 1 M NaCl, and placed at 4°C overnight. The lentivirus was precipitated by centrifuge at 5000 × *g* for 20 min at 4°C, re-suspended and store at −80°C before use. CG4 cells were cultured in OPC medium (DMEM/F12 supplemented with N2, B27, and 10 ng/ml PDGFA). After transfected with viruses, CG4 cells were cultured in OPC medium for 2 d to allow gene expression. Then cells were cultured in differentiation medium (DMEM/F12 supplemented with 2 ng/ml PDGFA, 40 ng/ml T3 or 50 ng/ml T4) for 6 d to differentiate. Cells were maintained at 37°C in a humidified incubator with 5% CO_2.

For Cas9-mediated Secisbp2l disruption in CG4 cells. Cas9-Secisbp2l plasmid was constructed by cloning spacer sequence targeting rat Secisbp2l at 5′-ggcggctggtcatg gggctG-3′ (note the G in uppercase means a variant nucleotide in CG4 cells that is different from T in GenBank GeneID 296115) into pSpCas9(bb)-2A-Neo (modified from Addgene plasmid #62988; Ran et al., 2013). Cas9-Secisbp2l plasmid was transfected into CG4 cells using FuGENE HD Transfection Reagent (Promega #E2311). The transfected CG4 cells were cultured in OPC medium supplemented with 200 μg/ml G418 (Sangon #A100859) for 4 d to kill nontransfected cells. The G418 resistant CG4 cells were then maintained in OPC medium. The primers gccttgttggatgtattcacc and agatacagcctccactgcag were used to amplify sequence flanking Cas9 target to evaluate mutation rate.

T4 and T3 measurement

P15 mouse brain and spinal cord tissues were dissected out in ice-cold PBS (1 ml for 100 mg wet weight tissue). The tissues were frozen and thawed twice, and then disrupted to homogenates by sonication. The homogenates were centrifuged at 5000 × *g* for 5 min at 4°C. Each 50 μl of supernatant was used for measurement of T4 and T3 concentrations with Mouse thyroxine T4 ELISA kit and Mouse Tri-iodothyronine T3 ELISA kit (CUSABIO), respectively.

CG4 cells infected with pCDH, pCDH-Secisbp2l, or treated with Cas9-Secisbp2l were cultured 6 d before harvesting. A total of 2×10^6 cells were centrifuged for each sample, re-suspended in 100 μl of PBS, and disrupted by sonication at 10% power for 12 s with Scientz-IID Ultrasonic Homogenizer (NingBo Scientz Biotechnology). After centrifugation, 90 μl of the sonicated solution was added to 10 μl of 500 ng/ml T4, and incubated at 37°C for 2 h. T3 and T4 concentrations were then measured by ELISA.

Western blotting

A sample containing 1× loading buffer was heated at 95°C for 5 min. A total of 20 μl of the sample was loaded onto an SDS-PAGE gel. The protein in the gel was then transferred to a PVDF membrane (Millipore, ISEQ00010). The membrane was blocked with 5% skimmed milk powder for 1 h at room temperature and incubated with the primary antibody overnight at 4°C. After washing three times with TBST, the

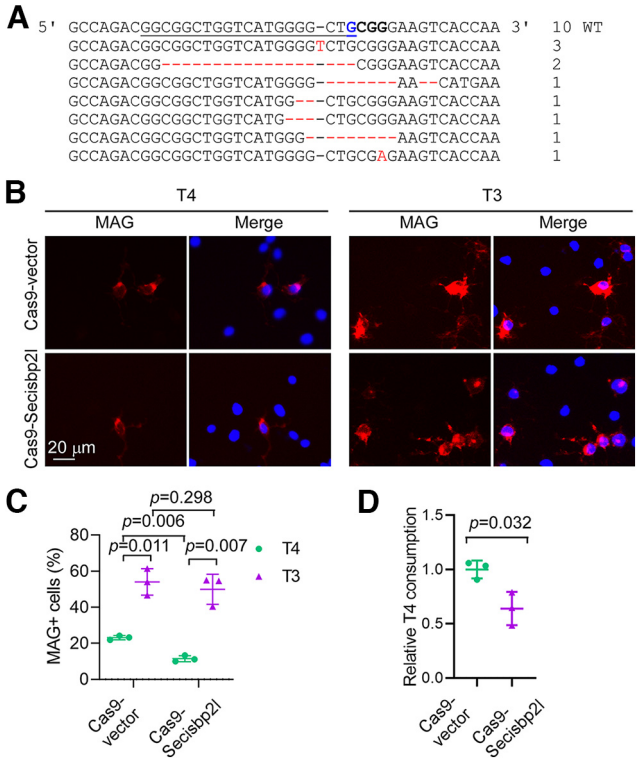

Figure 6. Disruption of Secisbp2l reduced T4-mediated differentiation of CG4 cells. ***A***, Cas9-mediated Secisbp2l mutation. 10 out of the 20 amplified DNA fragments contained the Secisbp2l mutation, indicating that ~50% of Secisbp2l in CG4 cells was mutated. The targeting sequence is underlined, and the PAM sequence is bolded. Note that the letter G in blue is variant from T in GenBank. ***B***, ***C***, Disruption of Secisbp2l reduced the differentiation of CG4 cells in response to T4 but not T3 treatment. ***D***, Altered T4 consumption activity in Secisbp2l-expressing or Secisbp2l-deficient CG4 cells. Data were showed as means ± SD; *t* test was used for statistical analysis based on triplicate results.

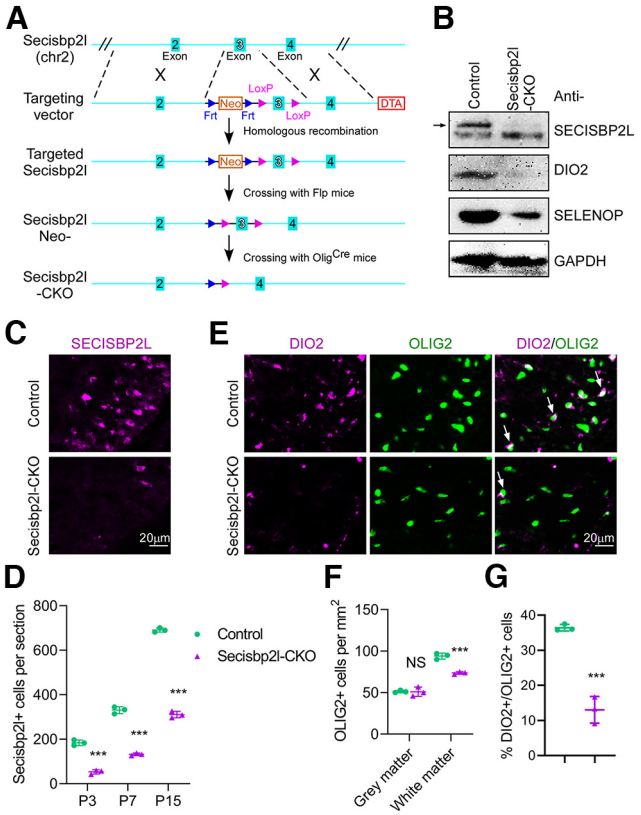

Figure 7. Secisbp2l CKO results in decreased selenoprotein levels. ***A***, Schematic representation of Secisbp2l-CKO generation. ***B***, Western blot confirmed that full-length SECISBP2L (indicated by an arrow) was absent in P3 Secisbp2l-CKO spinal cord, coupled with a dramatically reduced level of DIO2 and SELENOP. ***C***, ***D***, IF verified the loss of Secisbp2l+ cells in Secisbp2l-CKO mice from P3 to P15. ***E–G***, DIO2 was drastically reduced in OLIG2+ OLs in Secisbp2l-CKO as revealed by double immunostaining. All values are represented as mean ± SD; ***$p < 0.001$; NS, not significant.

membrane was probed with horseradish peroxidase (HRP)-conjugated secondary antibody (Promega) and then rinsed three times in TBST. Proteins were detected using an enhanced chemiluminescence (ECL) detection system (Thermo Scientific, catalog #32109) and x-ray film. The primary antibodies are used as follows: anti-SELENOP (Sant Cruz, sc-376858, 1:2000), GAPDH (Millipore, ABS16, 1:5000).

Experimental design and statistical analyses

Two-tailed *t* tests were used for statistical analysis within GraphPad Prism software.

Results

Secisbp2l is specifically upregulated in differentiating OLs and co-labeled with DIO2

To determine the roles of Secisbp2 and Secisbp2l in the regulation of Dio2 translation and local production of T3 during myelin development, we first analyzed their expression in the developing CNS tissue at both mRNA and protein levels. RNA ISH revealed that Secisbp2l, but not Secisbp2, was highly expressed in the spinal cord from E18.5 to P15 (Fig. 1*A*,*B*). The Secisbp2l-positive cells were largely confined to the white matter region, increased gradually in their numbers from E18.5 to P15 with a peak at P7 (Fig. 1*B*). Highly expression of Secisbp2l but not Secisbp2 was also detected in the white matter of cerebral cortex and cerebellum at P15 (Fig. 2*A*,*B*). These expression studies suggest that Secisbp2l is selectively expressed in glial cells at postnatal stages.

To accurately define the cell types that express Secisbp2l, we examined the co-expression of SECISBP2L with markers for both astrocytes and oligodenrocytes in P7 spinal cord tissues. A polyclonal anti-SECISBP2L antibody was developed and extensively verified by comparison to anti-FLAG or Sigma Prestige Antibodies anti-SECISBP2L (Fig. 3*A*,*C*). Double immunostaining experiments showed that SECISBP2L co-labeled with the differentiating OL markers NKX2.2 and CC1 and the mature OL marker MBP (Fig. 1*C*), but not with astrocyte marker GFAP or the immature OPC marker Pdgfra (Fig. 1*C*). In fact, the expression of Secisbp2l is nearly identical to that of CC1, with ~95% CC1-expressing cells positive for SECISBP2L and 98% SECISBP2L-expressing cells positive for CC1 (Fig. 1*D*). The specific expression of Secisbp2l in differentiating OLs was further confirmed by its dramatic reduction in P3 spinal tissues of Olig1−/− KO and Nkx2.2 CKO mice (Fig. 2*C*) with impaired OL differentiation (Qi et al., 2001; Lu et al., 2002). Co-expression of SECISBP2L and CC1 was also conspicuous in the white matter OLs in P15 cerebellum and cortex (Fig. 1*F*).

Previous studies found that mRNA of DIO2, the major selenoprotein implicated in T3 production in the CNS, is primarily expressed in astrocytes (Guadaño-Ferraz et al., 1997, 1999). However, considering the abundant expression of SECISBP2L in

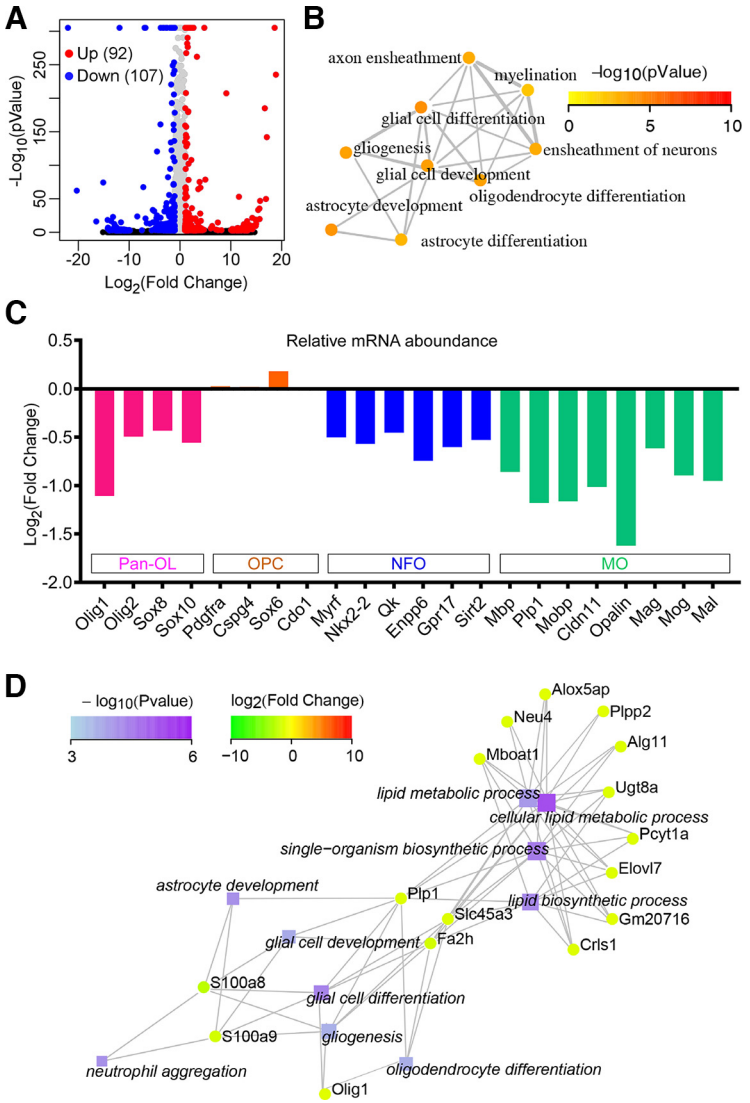

Figure 8. Expression of OL differentiation genes is downregulated in Secisbp2l-CKO mice. ***A***, Volcano plot of differentially expressed genes. A value of 303 was assigned for -Log_{10}(pValue) larger than 302 (Extended Data Fig. 8-1). ***B***, Expression of OL differentiation genes and myelin-related genes was significantly enriched in downregulated genes as revealed by gene ontology analysis in Secisbp2l-CKO mice. ***C***, Expression analysis of pan OL lineage cell (Pan-OL), OL precursor cell (OPC), newly formed OL (NFO), and mature OL (MO) markers. ***D***, Gene ontology analysis of the downregulated genes in Secisbp2l mutants. Glial cell development and lipid metabolism were the most affected biological processes.

OLs and undetectable expression of SECISBP2 in the CNS, we raise a question that SECISBP2L may act as an essential factor for full-length DIO2 protein translation in OLs. We next examined whether DIO2 is similarly expressed in differentiating OLs. For this purpose, we developed a polyclonal antibody against the C-terminal peptides of DIO2 protein. Anti-DIO2 specificity was validated by Western blotting (Fig. 3*B*). Double labeling experiments established that full-length active DIO2 was indeed co-expressed in CC1+ NFOs in P7 spinal cord tissues (Fig. 1*E*,*F*). The simultaneous expression of SECISBP2L and DIO2 proteins in NFOs strongly suggests that SECISBP2L regulates DIO2 translation and T3 production that facilitates OL differentiation and maturation.

Secisbp2l promotes DIO2 translation and CG4 cell differentiation

To further test the idea that Secisbp2l can stimulate DIO2 translation, we next studied whether SECISBP2L protein can directly bind to the SECIS elements of Dio1-3 mRNAs that are transcribed in brain tissues (Fig. 4*A*). Co-immunoprecipitation experiments revealed that, compared with the negative control Actb (β-actin), Dio2, and Dio3 mRNAs were highly enriched from anti-SECISBP2L immunoprecipitates of spinal cord tissues (Fig. 4*B*).

The co-precipitation of Dio2 mRNA and SECISBP2L protein has raised the possibility that Secisbp2l directly promotes Dio2 translation in the CNS. To test this possibility, we developed a dual luciferase assay to examine how SECISBP2L impacts the translation of selenoprotein mRNAs. A SecCHECK vector was constructed from siCHECK-2 (Promega) plasmid in which a TGC codon was changed into TGA stop codon by site-directed mutagenesis (Fagegaltier et al., 2000), causing a Cys258Sec mutation of the firefly luciferase (Luc; Fig. 4*C*). SECIS element from Dio1, Dio2, and Dio3 was then inserted into SecCHECK at the 3′-UTR of Luc to obtain Dio1-SECIS, Dio2-SECIS and Dio3-SECIS, respectively (Fig. 4*C*). Consistent with the previous results that C-terminal fragment of SECISBP2 (CT-SECISBP2) but not CT-SECISBP2L could facilitate selenoprotein translation (Copeland et al., 2000, 2001; Donovan and Copeland, 2009, 2012), expression of the Secisbp2l C-terminal fragment (CT-Secisbp2l) alone did not enhance Luc activity in HEK293T cells (Fig. 4*D*). However, expression of full-length SECISBP2L significantly increased the Luc activity to the same extent of SECISBP2 in Dio1-SECIS, Dio2-SECIS, and Dio3-SECIS construct as compared with the control vector (Fig. 4*D*). The results suggested that different from SECISBP2, the N terminus is required for the full activity of SECISBP2L in selenoprotein translation.

Previous studies have demonstrated that eEFSec is a selenoprotein-specific elongation factor that interacts with CT-SECISBP2 and is essential for selenoprotein translation (Fagegaltier et al., 2000; Gonzalez-Flores et al., 2012). Therefore, we next explored whether SECISBP2L protein could directly interact with eEFSec. Because the efficiency of over-expressing full-length Secisbp2l was too low in our co-transfection experiments (Fig. 5*A*), the split mCherry strategy was therefore used to test their interaction (Fan et al., 2008). The split mCherry halves could not form a functional fluorescent protein unless there is an interaction between the fused proteins (Fig. 5*B*). Secisbp2, Secisbp2l and CT-Secisbp2l were fused with C-terminal half of mCherry, whereas eEFSec was fused with N-terminal half of mCherry (Fig. 5*C*). Strong mCherry fluorescence was detected with both full-length Secisbp2 and Secisbp2l, but not with the CT-Secisbp2l (Fig. 5*D*), indicating that full-length Secisbp2l is capable of interacting with eEFSec within cells. Since there was difficulty in

expressing full-length Secisbp2 and Secisbp2l proteins, only the CT-SECISBP2 and CT-SECISBP2L fragments were used to test their functions in selenoprotein translation (Copeland et al., 2000, 2001; Donovan and Copeland, 2009, 2012). Our results revealed that the full-length SECISBP2L but not its C-terminal fragment was able to recruit eEFSec to recode the UGA into Sec, which also explained why SECISBP2L's function in selenoprotein translation was not discovered previously.

When Secisbp2l was mutated by Cas9-mediated gene mutation, differentiation of CG-4 cells was significantly reduced in differentiation medium containing only T4, in agreement with the lack of T4 conversion to T3 when Secisbp2l was disrupted. However, the Secisbp2l mutant CG4 cells differentiated normally in T3-containing medium (Fig. 6*A–C*). Moreover, Secisbp2l KO cells decreased T4 consumption as measured by ELISA (Fig. 6*D*). Together, these results indicated that Secisbp2l expression is capable of facilitating DIO2 translation by binding to its SECIS element, enhancing the T4-to-T3 conversion and promoting terminal differentiation of CG-4 cells.

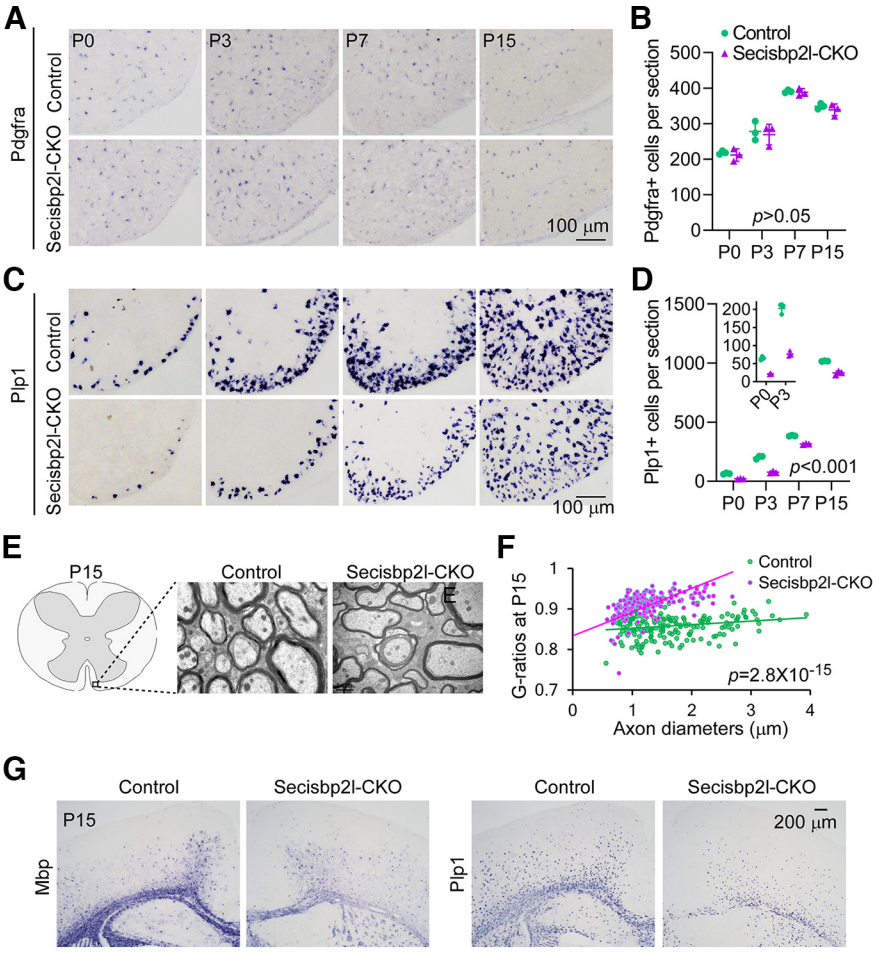

Figure 9. Secisbp2l-CKO causes reduced OL differentiation and myelin deficit. ***A–D***, ISH revealed a normal number of Pdgfra+ OPC in Secisbp2l-CKO mice from P0 to P15 (***A***, ***B***), but the number of mature Plp1+OLs is significantly reduced at all tested stages (***C***, ***D***). Values are represented as mean ± SD (***B***, ***D***). ***E***, ***F***, Transmission electron microscopy of P15 spinal cord showed thinner myelin sheaths in Secisbp2l-CKO mice (***E***) and increased G-ratios (***F***), G-ratios were calculated from pooled data from three animals for both control and Secisbp2l-CKO mice. ***G***, Decreased differentiation of OL in brain tissues from Secisbp2l CKO mice. ISH revealed a reduced expression of the mature OL markers Mbp and Plp1 in Secisbp2l-CKO mice.

Secisbp2l CKO mice exhibit deficits in selenoprotein translation, myelination and locomotion

To elucidate the *in vivo* function of Secisbp2l in OL differentiation, we created the Olig1^{cre};Secisbp2l$^{flox/flox}$ CKO mice for specific disruption of its function in OL lineage (Fig. 7*A*). Western blotting confirmed that expression of SECISBP2L and DIO2 proteins was largely lost in CKO spinal cord tissue. As a control, expression of SELENOP (also known as SEPP1), an OL-abundant selenoprotein (Zhang et al., 2014), was also markedly reduced (Fig. 7*B*). Immunofluorescent staining confirmed the dramatic reduction of SECISBP2L+ and DIO2+/Olig2+ OLs in the white matter of mutant tissues (Fig. 7*C–G*).

Transcriptome analysis identified 92 significantly upregulated genes versus 107 downregulated genes in Secisbp2l-CKO tissues (Fig. 8*A*; Extended Data Fig. 8-1). Gene ontology analysis of the downregulated genes revealed the enrichment of genes that are primarily involved in OL differentiation and myelination (Fig. 8*B–D*). Noticeably, expression of NFO and mature OL markers (e.g., Mbp, Plp1, Opalin, etc.) was all downregulated in Secisbp2l-CKO mice ($p < 0.01$, $q < 0.01$; Fig. 8*C*). Consistently, pan-OL lineage genes (Olig1, Olig2, Sox8, and Sox10) that are expressed in both OPCs and mature OLs were similarly downregulated (Fig. 8*C*). As a reference control, expression of motoneuron-related and astrocyte-related genes was not significantly altered (data not shown). Together, these gene expression analyses indicated a selective impediment of OL differentiation when Secisbp2l expression was conditionally deleted in OL lineage.

OL differentiation in Secisbp2l-CKO mice was also corroborated at the tissue level by RNA ISH. Consistent with the transcriptome analyses, Secisbp2l mutation did not affect the expression of OPC marker Pdgfra in the spinal cord of Secisbp2l-CKO (Fig. 9*A*,*B*). However, the number of Plp1+ mature OLs was significantly lower in Secisbp2l-CKO from P0 to P15 (Fig. 9*C*,*D*). Similarly, expression of Plp1 and Mbp was also decreased in the white matter of cortex (corpus callosum) of Secisbp2l-CKO mice (Fig. 9*G*). To confirm that Secisbp2l functions autonomously in OL lineage, we generated another OL-specific Secisbp2l mutant line with Cnp-Cre mice, and an astrocyte-specific mutant line with mGfap-Cre line. Phenotypic analyses demonstrated that expression of Mbp and Plp1 was significantly downregulated in Cnp-Cre;Secisbp2l-CKO mice, but remained normal in mGfap-Cre;Secisbp2l-CKO mice (Fig. 10). These results provided additional evidence that the intrinsic Secisbp2l expression OL cells is required for their terminal differentiation.

We next examined myelin structures in Secisbp2l-CKO mutant mice. Ultrastructural analyses under transmission electronic microscope demonstrated that myelin sheaths in the white matter of P15 spinal cord in Secisbp2l-CKO mice were significantly

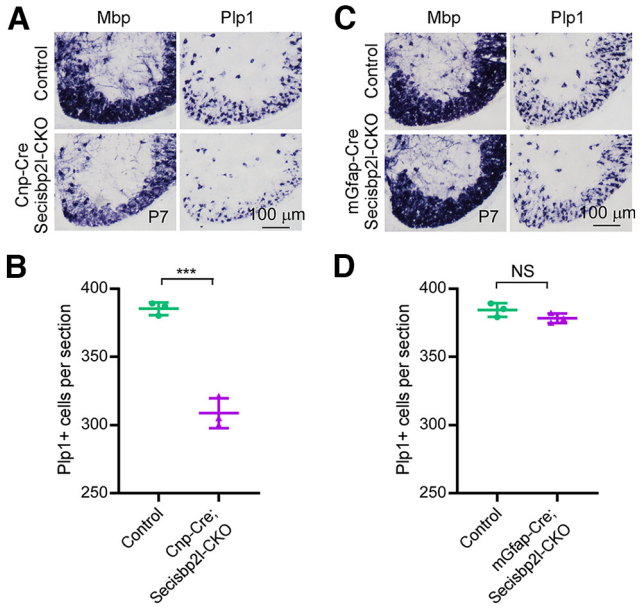

Figure 10. Impaired differentiation of OLs in Cnp-Cre;Secisbp2l-CKO mice but not in mGfap-Cre;Secisbp2l-CKO mice. ***A***, ***B***, ISH revealed a decreased expression of the mature OL markers Mbp and Plp1 in Cnp-Cre;Secisbp2l-CKO mice. ***C***, ***D***, The expression of Mbp and Plp1 remained normal in mGfap-Cre;Secisbp2l-CKO. ***$p<0.001$; NS, not significant.

Movie 1. P15 control (left) and Secisbp2l-CKO (right) mice hanging by tails. [View online]

thinner than those in the WT tissues. Statistical analyses of >180 myelinated axons unraveled an increased g-ratio in the mutant tissues (Fig. 9*E*,*F*). Tail suspension assays revealed strong body trembling in Secisbp2l-CKO mice at P15, and this tremor phenotype remained evident in Secisbp2l-CKO mice as late as P45 (Movies 1, 2). Therefore, conditional deletion of Secisbp2l in OL lineage caused significant hypomyelination and a locomotive deficit in the mutant animals.

Defective OL differentiation in Secisbp2l-CKO mice can be rescued by T3 analog but not T4

As translation of Dio2 in OLs was disrupted by Secisbp2l-CKO (Fig. 7*B*), it is expected that Secisbp2l mutation would lead to a compromised T4-to-T3 conversion. To confirm this idea, we performed ELISA assays to determine the T4 and T3 concentration in the brain and spinal cord lysates. Indeed, T4 level was elevated in the brain and spinal tissues of Secisbp2l-CKO mice compared with those of control mice, while T3 was significantly decreased in the mutants (Fig. 11*A*). Considering that OLs only constitute a small portion of CNS tissue, this result likely underestimated the robustness of T4 to T3 conversion in differentiating OLs associated

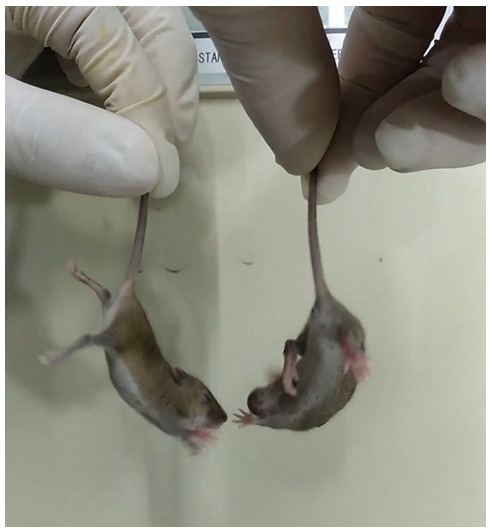

Movie 2. P45 control (left) and Secisbp2l-CKO (right) mice hanging by tails. [View online]

with the strong upregulation of SECISBP2L protein expression (Fig. 1).

To directly test the notion that the myelin phenotypes observed in Secisbp2l-CKO mice are caused by the impaired T4-to-T3 conversion, we next examined the rescue effects of T3 and T4 compounds on defective OL differentiation in the mutants. In normal mice, injection of either T4 or GC-1 (T3 analog) from P0 to P3 was able to enhance Mbp and Plp1 expression as compared with PBS control (Fig. 11*C*). However, in Secisbp2l-CKO animals, only GC-1 but not T4 had the stimulatory effect on OL differentiation (Fig. 11*D*). Therefore, the exogenous administration of T3 hormone analog, but not T4 precursor compound, can rescue defective OL differentiation in Secisbp2l-CKO mutants with impaired DIO2 expression and T4-to-T3 conversion. These findings further establish that Secisbp2l is involved in the autonomous regulation of OL differentiation (Fig. 11*E*).

Discussion

Secisbp2 is the first cloned eukaryotic SECIS binding protein gene (Copeland et al., 2000). The same study also identified its homologous gene Secisbp2l encodes a SECIS binding protein (Copeland et al., 2000). Although both SECISBP2 and SECISBP2L can bind to SECIS elements, only SECISBP2 was demonstrated to be able to facilitate decoding UGA into Sec (Copeland et al., 2000, 2001; Donovan and Copeland, 2009, 2012). SECISBP2L was thus considered to be unable to substitute SECISBP2's function in selenoprotein translation (Copeland et al., 2000, 2001; Donovan and Copeland, 2009, 2012). However, because of the difficulty in expression of the full-length SECISBP2 and SECISBP2L proteins, all the previous studies used their C-terminal fragments in cell free translation system to examine their function, which may cover up SECISBP2L's role in selenoprotein translation. In this study, we found that the full-length SECISBP2L protein is also capable of promoting the translation of selenoproteins in an SECIS-dependent manner (Fig. 4). Moreover, our studies showed that contrary to SECISBP2 whose N terminus is dispensable, the N terminus of SECISBP2L is required to recruit eEFSec for UGA to Sec recoding (Fig. 5).

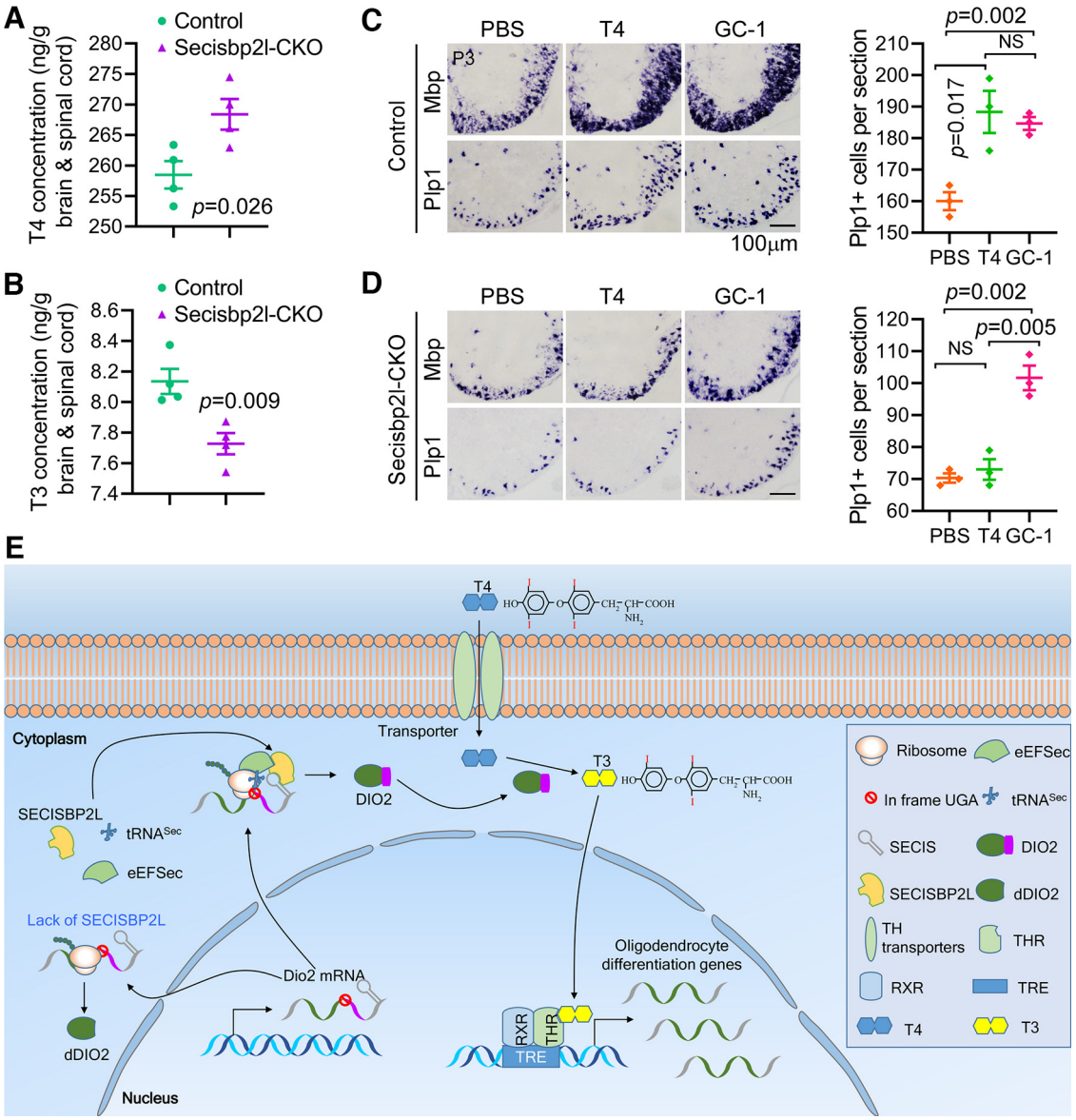

Figure 11. GC-1 but not T4 partially rescues OL differentiation in Secisbp2l-CKO mice. ***A***, ***B***, Increased T4 and decreased T3 levels in the CNS of Secisbp2l-CKO mice. T4 and T3 levels were measured at P15 from four pairs of control and Secisbp2l-CKO mice. ***C***, Injection of both T4 and GC-1 from P0 to P3 promotes OL differentiation in control mice. ***D***, Only GC-1 injection promotes OL differentiation in Secisbp2l-CKO mice. All values are represented as means ± SD. ***E***, Autonomous regulation of OL differentiation by SECISBP2L. In the absence of SECISBP2L, DIO2 translation is terminated by in-frame UGA stop codon in Dio2 mRNA, resulting in a catalytically dead Dio2 (dDIO2) protein. When SECISBP2L is expressed in differentiating OLs, it helps to decode the UGA into Sec for translation of full-length DIO2 protein, which in turn converts T4 into T3 to enhance OL differentiation.

Previous studies demonstrated that T3 production and secretion from thyroid gland are inhibited in Dio1 KO and Sec-tRNA CKO mice but circulating T3 in blood remains normal (Schneider et al., 2006; Chiu-Ugalde et al., 2012), suggesting that the majority of T3 is locally produced by organs that require a high level of T3. In the CNS, as Dio1 expression is not detectable, the generation of T3 is thought to be largely dependent on Dio2 (Guadaño-Ferraz et al., 1997, 1999; St Germain et al., 2009; Arrojo and Bianco, 2011). It was previously reported that Dio2 mRNA is primarily expressed by astrocytes. Since astrocytes also express TH transporters, they have been considered as the major source for T4-to-T3 conversion and T3 exportation to other neural cells including OLs (Calzà et al., 2015). However, the present study discovered that full-length active DIO2 protein is highly expressed in OLs, but not in astrocytes (Fig. 1*E*). More importantly, we found that Secisbp2l is also predominantly expressed in OLs (Fig. 1) and its mutation in OLs decreased the production of both DIO2 and TH in the CNS tissue (Figs. 4*B*, 11*A*,*B*), indicating that OLs are not only T3 consumers, but also T3 producers. The impeded OL differentiation and hypomyelination in Secisbp2l-CKO mutants also suggests that the endogenous T3 production in OLs provides a positive autonomous feedback to enhance or reinforce their terminal differentiation. Considering that Secisbp2l, but not Secisbp2, is specifically and highly expressed in differentiating OLs (Fig. 1), we postulate that Secisbp2l is the major SECIS binding protein in DIO2 synthesis and T3 production in OLs (Fig. 11*E*). However, Secisbp2l may also contribute to the regulation of selenium level in the CNS, because SELENOP, a multiple selenocysteine-containing protein involved in selenium homeostasis maintenance, was significantly reduced in the spinal cord of Secisbp2l-CKO mice (Fig. 7*B*). Thus, Secisbp2l's function in other selenoprotein translation and

their function in differentiation and myelination of OLs remain to be determined in future studies.

In sum, the present study has presented the first line of evidence that Secisbp2l is selectively and robustly expressed in differentiating OLs and is capable of decoding the "UGA" stop codon into Sec necessary for DIO2 biosynthesis. Through controlled expression of Secisbp2l for DIO2 translation and T3 production, OLs can self-regulate their differentiation and myelinogenesis, and possibly contribute to the maintenance of TH homeostasis in the CNS tissue as well. The current study has also uncovered a novel phenomenon of autonomous regulation of cell differentiation in OLs and unraveled the molecular mechanism underlying this positive feedback process.

References

Arrojo EDR, Bianco AC (2011) Type 2 deiodinase at the crossroads of thyroid hormone action. Int J Biochem Cell Biol 43:1432–1441.

Baas D, Legrand C, Samarut J, Flamant F (2002) Persistence of oligodendrocyte precursor cells and altered myelination in optic nerve associated to retina degeneration in mice devoid of all thyroid hormone receptors. Proc Natl Acad Sci U S A 99:2907–2911.

Barres BA, Lazar MA, Raff MC (1994) A novel role for thyroid hormone, glucocorticoids and retinoic acid in timing oligodendrocyte development. Development 120:1097–1108.

Baxi EG, Schott JT, Fairchild AN, Kirby LA, Karani R, Uapinyoying P, Pardo-Villamizar C, Rothstein JR, Bergles DE, Calabresi PA (2014) A selective thyroid hormone β receptor agonist enhances human and rodent oligodendrocyte differentiation. Glia 62:1513–1529.

Bernal J (2017) Thyroid hormone regulated genes in cerebral cortex development. J Endocrinol 232:R83–R97.

Bianco AC, Kim BW (2006) Deiodinases: implications of the local control of thyroid hormone action. J Clin Invest 116:2571–2579.

Billon N, Jolicoeur C, Tokumoto Y, Vennström B, Raff M (2002) Normal timing of oligodendrocyte development depends on thyroid hormone receptor alpha 1 (TRalpha1). EMBO J 21:6452–6460.

Calzà L, Fernandez M, Giardino L (2010) Cellular approaches to central nervous system remyelination stimulation: thyroid hormone to promote myelin repair via endogenous stem and precursor cells. J Mol Endocrinol 44:13–23.

Calzà L, Fernández M, Giardino L (2015) Role of the thyroid system in myelination and neural connectivity. Compr Physiol 5:1405–1421.

Chiu-Ugalde J, Wirth EK, Klein MO, Sapin R, Fradejas-Villar N, Renko K, Schomburg L, Köhrle J, Schweizer U (2012) Thyroid function is maintained despite increased oxidative stress in mice lacking selenoprotein biosynthesis in thyroid epithelial cells. Antioxid Redox Signal 17:902–913.

Copeland PR, Fletcher JE, Carlson BA, Hatfield DL, Driscoll DM (2000) A novel RNA binding protein, SBP2, is required for the translation of mammalian selenoprotein mRNAs. EMBO J 19:306–314.

Copeland PR, Stepanik VA, Driscoll DM (2001) Insight into mammalian selenocysteine insertion: domain structure and ribosome binding properties of Sec insertion sequence binding protein 2. Mol Cell Biol 21:1491–1498.

Donovan J, Copeland PR (2009) Evolutionary history of selenocysteine incorporation from the perspective of SECIS binding proteins. BMC Evol Biol 9:229.

Donovan J, Copeland PR (2012) Selenocysteine insertion sequence binding protein 2L is implicated as a novel post-transcriptional regulator of selenoprotein expression. PLoS One 7:e35581.

Dugas JC, Ibrahim A, Barres BA (2012) The T3-induced gene KLF9 regulates oligodendrocyte differentiation and myelin regeneration. Mol Cell Neurosci 50:45–57.

Dumitrescu AM, Refetoff S (2013) The syndromes of reduced sensitivity to thyroid hormone. Biochim Biophys Acta 1830:3987–4003.

Fagegaltier D, Hubert N, Yamada K, Mizutani T, Carbon P, Krol A (2000) Characterization of mSelB, a novel mammalian elongation factor for selenoprotein translation. EMBO J 19:4796–4805.

Fan JY, Cui ZQ, Wei HP, Zhang ZP, Zhou YF, Wang YP, Zhang XE (2008) Split mCherry as a new red bimolecular fluorescence complementation system for visualizing protein-protein interactions in living cells. Biochem Biophys Res Commun 367:47–53.

Farley FW, Soriano P, Steffen LS, Dymecki SM (2000) Widespread recombinase expression using FLPeR (flipper) mice. Genesis 28:106–110.

Gonzalez-Flores JN, Gupta N, DeMong LW, Copeland PR (2012) The selenocysteine-specific elongation factor contains a novel and multi-functional domain. J Biol Chem 287:38936–38945.

Guadaño-Ferraz A, Obregón MJ, St Germain DL, Bernal J (1997) The type 2 iodothyronine deiodinase is expressed primarily in glial cells in the neonatal rat brain. Proc Natl Acad Sci U S A 94:10391–10396.

Guadaño-Ferraz A, Escámez MJ, Rausell E, Bernal J (1999) Expression of type 2 iodothyronine deiodinase in hypothyroid rat brain indicates an important role of thyroid hormone in the development of specific primary sensory systems. J Neurosci 19:3430–3439.

Hamburgh M (1966) Evidence for a direct effect of temperature and thyroid hormone on myelinogenesis in vitro. Dev Biol 13:15–30.

Kryukov GV, Castellano S, Novoselov SV, Lobanov AV, Zehtab O, Guigó R, Gladyshev VN (2003) Characterization of mammalian selenoproteomes. Science 300:1439–1443.

Lee JY, Petratos S (2016) Thyroid hormone signaling in oligodendrocytes: from extracellular transport to intracellular signal. Mol Neurobiol 53:6568–6583.

Lu QR, Sun T, Zhu Z, Ma N, Garcia M, Stiles CD, Rowitch DH (2002) Common developmental requirement for Olig function indicates a motor neuron/oligodendrocyte connection. Cell 109:75–86.

Picou F, Fauquier T, Chatonnet F, Flamant F (2012) A bimodal influence of thyroid hormone on cerebellum oligodendrocyte differentiation. Mol Endocrinol 26:608–618.

Qi Y, Cai J, Wu Y, Wu R, Lee J, Fu H, Rao M, Sussel L, Rubenstein J, Qiu M (2001) Control of oligodendrocyte differentiation by the Nkx2.2 homeodomain transcription factor. Development 128:2723–2733.

Ran FA, Hsu PD, Wright J, Agarwala V, Scott DA, Zhang F (2013) Genome engineering using the CRISPR-Cas9 system. Nat Protoc 8:2281–2308.

Schneider MJ, Fiering SN, Thai B, Wu SY, St Germain E, Parlow AF, St Germain DL, Galton VA (2006) Targeted disruption of the type 1 selenodeiodinase gene (Dio1) results in marked changes in thyroid hormone economy in mice. Endocrinology 147:580–589.

Sharlin DS, Tighe D, Gilbert ME, Zoeller RT (2008) The balance between oligodendrocyte and astrocyte production in major white matter tracts is linearly related to serum total thyroxine. Endocrinology 149:2527–2536.

St Germain DL, Galton VA, Hernandez A (2009) Minireview: defining the roles of the iodothyronine deiodinases: current concepts and challenges. Endocrinology 150:1097–1107.

Sun S, Huang H, Qi YB, Qiu M, Dai ZM (2015) Complementary annealing mediated by exonuclease: a method for seamless cloning and conditioning site-directed mutagenesis. Biotechnol Biotechnol Equip 29:105–110.

Vose LR, Vinukonda G, Jo S, Miry O, Diamond D, Korumilli R, Arshad A, Zia MT, Hu F, Kayton RJ, La Gamma EF, Bansal R, Bianco AC, Ballabh P (2013) Treatment with thyroxine restores myelination and clinical recovery after intraventricular hemorrhage. J Neurosci 33:17232–17246.

Zhang Y, Chen K, Sloan SA, Bennett ML, Scholze AR, O'Keeffe S, Phatnani HP, Guarnieri P, Caneda C, Ruderisch N, Deng S, Liddelow SA, Zhang C, Daneman R, Maniatis T, Barres BA, Wu JQ (2014) An RNA-sequencing transcriptome and splicing database of glia, neurons, and vascular cells of the cerebral cortex. J Neurosci 34:11929–11947.